Analytica Chimica Acta 1217 (2022) 340009

Contents lists available at ScienceDirect

Analytica Chimica Acta

journal homepage: www.elsevier.com/locate/aca

Rapid RNA detection through intra-enzyme chain replacement-promoted Cas13a cascade cyclic reaction without amplification

Hongwei Zeng [a], Penghui Zhang [b], Xue Jiang [a], Changyuan Duan [a], Yang Yu [a], Qiaoming Wu [a], Xiaolan Yang [a,*]

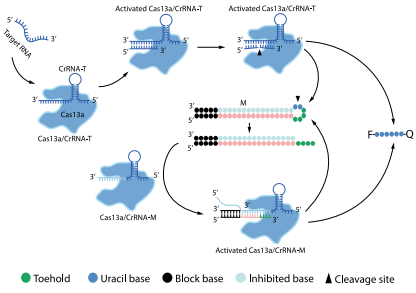
[a] Key Laboratory of Clinical Laboratory Diagnostics (Ministry of Education), College of Laboratory Medicine, Chongqing Medical University, Chongqing, 400016, PR China

[b] Clinical Laboratory Center, Ministry of Education Key Laboratory of Child Development Diseases and Disorders, Key Laboratory of Pediatrics in Chongqing, Chongqing International Science and Technology Cooperation Center for Child Development and Disorders, Children's Hospital, Chongqing Medical University, Chongqing, PR China

HIGHLIGHTS

- An intra-enzyme chain replacement-promoted Cas13a cascade cyclic signal enhancement strategy without amplification is proposed.
- "mix & read at room temperature" mode expanded POCT application of Cas13a.
- Analyses of the clinical RSV samples demonstrate good performance of proposed strategy.

GRAPHICAL ABSTRACT



ARTICLE INFO

Keywords:
CRISPR-Cas13a cascade cyclic rapid test room temperature respiratory syncytial virus

ABSTRACT

The clinical methods to detect RNA viruses and disease-related RNAs suffer from time-consuming processes, high false-positive rates, or limited sensitivity. Here, we propose a strategy for rapid RNA detection through intra-enzyme chain replacement-mediated Cas13a cascade cyclic reaction without target amplification. A hairpin RNA mediator (a cleavage substrate for target-activated Cas13a) and a guiding RNA recognized by the cleavage product through intra-enzyme chain replacement were designed and optimized. Upon the recognition and binding of the target RNA to the Cas13a/CrRNA complex, Cas13a is initially activated to cleave the mediator, and the cleavage products recognize the corresponding Cas13a/CrRNA complex by intra-enzyme chain replacement and initiate the circular cascade of Cas13a cleavage and activation. The accumulated active Cas13a cleaves fluorescent reporter probe for achieving target RNA detection. This "mix & read" RNA detection at room temperature was performed in total 30 min. Using miRNA-21 as the target, the changes in fluorescence intensity were linearly correlated to the concentrations from 10 fM to 50 pM with the detection limit of 75 aM, while no significant changes in fluorescence intensity were detected for non-targets. This method applied to the clinical sputum respiratory syncytial virus-positive samples gave results consistent with those from the clinical

Abbreviations: CRISPR, clustered regularly interspaced short palindromic repeats; Cas, caspase; CrRNA, CRISPR guide RNA; Cpccc, intra-enzyme chain replacement-promoted Cas13a cascade cyclic reaction; LOD, limit of detection; miRNA, microRNA; PCR, polymerase chain reaction; RSV, respiratory syncytial virus; SDS-PAGE, sodium dodecyl sulfate-polyacrylamide gel electrophoresis.

* Corresponding author.
E-mail address: xiaolanyang666@cqmu.edu.cn (X. Yang).

https://doi.org/10.1016/j.aca.2022.340009
Received 6 December 2021; Received in revised form 12 May 2022; Accepted 26 May 2022
Available online 31 May 2022
0003-2670/© 2022 Elsevier B.V. All rights reserved.

fluorescence immunoassay. Thus, intra-enzyme chain replacement-promoted Cas13a cascade cyclic reaction for detection of RNA viruses in the "mix & read" mode at room temperature is rapid, simple, convenient, and efficient for RNA detection and can be adapted to point-of-care testing for high throughput screening of RNA virus infections.

1. Introduction

RNAs, including non-coding RNAs, such as microRNAs (miRNAs), circular RNAs, and long non-coding RNAs, have critical roles in regulating gene expression and metabolism [1–4]. Thus, the occurrence and progression of diseases are associated with the dysregulation of RNAs. Infections with RNA viruses, including SARS-CoV-2, hepatitis C virus, influenza virus, severe acute respiratory syndrome-associated coronavirus, Middle East respiratory syndrome coronavirus, and Ebola virus, adversely affect human health [5–10]. Additionally, RNA virus-associated epidemics are a substantial threat to public health. Nucleic acid analysis using advanced molecular biology techniques is the gold standard for detecting pathogens, including RNA viruses [11,12]. In contrast to DNA, RNA is usually unstable and susceptible to mutation [13]. Thus, a rapid, simple, and sensitive method for RNA detection is critical for the early diagnosis of diseases and the management of pathogen epidemics [14,15].

The gold standard technique for RNA detection based on polymerase chain reaction (PCR) is widely used in clinical practice. However, PCR-based RNA detection involves reverse transcription, followed by repeated denaturation, annealing, and extension; it is laborious, cost expensive, and time consuming with the need for bulky equipment and skilled technicians [16]. Recently, various isothermal amplification methods for RNA detection, such as rolling circle amplification (RCA), isothermal exponential amplification reaction (EXPAR), and nucleic acid sequence-based amplification (NASBA), have been developed [17–20]. However, these methods also involve complex systems, tedious experimental steps, various enzymes, and complex probe design [21].

The newly developed clustered regularly interspaced palindrome repeat (CRISPR)-Caspase (Cas) gene splicing system can efficiently cleave the reporter single-stranded nucleic acids after the specific binding of a target sequence to the guide RNA of CRISPR (CrRNA), which leads to the quantitative activation of Cas [22–24]. The target-specific quantitative activation of Cas and highly efficient non-specific cleavage of a reporter RNA have enabled the CRISPR-Cas gene splicing systems to achieve highly sensitive and specific detection of nucleic acids [25]. Cas9, Cas12a, and Cas14 specifically recognize DNA, whereas Cas13a specifically recognizes RNA [26–28]. In 2018, Feng Zhang reported the "SHERLOCK" system for RNA detection and Jennifer proposed the "DETECTR" system for DNA detection [29,30]. The "SHERLOCK" and "DETECTR" systems utilize preceding isothermal amplification of target coupled with CRISPR-Cas13a and CRISPR-Cas12a, respectively. However, the coupled isothermal amplification system is complex and time consuming [31]. Previous studies have reported some microfluidic systems using CRISPR-Cas for miRNA detection, but the sensitivity of these systems is limited [32,33]. To enhance the sensitivity of Cas-based nucleic acid detection, the target RNA is currently amplified ahead of Cas-induced cleavage. This method is time consuming and requires specialized equipment and skilled technicians [34–40]. In 2021, Kai Shi first proposed a CRISPR-Cas12-driven feedback amplification for the super-sensitive detection of DNA with a limit of detection (LOD) of 5.0 aM [41]. The author designed a switchable-caged RNA sequence locked by a DNA strand as the substrate and an assistant target DNA. The Cas-mediated cleavage of the switchable-caged RNA sequence promotes the formation of CrRNA, which subsequently hybridizes with the designed assistant target DNA to drive the feedback amplification. However, the time required for this CRISPR-Cas12-driven feedback amplification is as high as 4 h because of CrRNA designed as the trigger needing an additional assembly process between CrRNA and Cas12a. Moreover, this strategy is just aimed at DNA detection and can't detect RNA target. To the best of our knowledge, methods for RNA detection without PCR amplification of the target with short analysis time, low cost, high sensitivity, and simple operation steps are currently not available.

In this study, a new method based on intra-enzyme chain replacement-promoted Cas13a cascade cyclic reaction (Cpccc) for the rapid detection of RNA was developed without target amplification. The enhanced selectivity, sensitivity, short analysis duration, easy manipulation and feasibility of "mix & read" of the method were demonstrated using miRNA-21 as the model. Additionally, the clinical application performance of Cpccc was evaluated using the clinical respiratory syncytial virus (RSV) sputum specimens.

2. Materials and methods

2.1. Materials and apparatus

All involved DNA, target miRNAs, double-labeled reporter RNA probe modified with 5′-fluorescent (FAM) and 3′-quencher (BHQ1) were synthesized and purified by Sangon Biotechnology Co., Ltd. (Shanghai, China). Detailed sequence information and modification were listed in Table S1. T7 RNA polymerase and the NTP mix were purchased from New England Biolabs (Beijing, China). Recombinant RNase inhibitor, recombinant DNase I (RNase-free), diethylpyrocarbonate (DEPC), DNA Ladder (20 bp) were purchased from Takara Biotechnology Co., Ltd. (Dalian, China). The RNA purification kit was purchased from Tiangen Biotech Co., Ltd. (Beijing, China). Chloramphenicol, glycerol, kanamycin, imidazole and other chemicals were purchased from Sangon Biotechnology Co., Ltd. (Shanghai, China).

Gel image was recorded on an imaging system (Bio-Rad Laboratories, USA). The fluorescence measurements were achieved by Rotor-Gene Q real-time fluorescence quantitative PCR instrument (QIAGEN, Germany).

2.2. Cas13a expression and purification

The LbuCas13a-loading plasmid pET-28a-LbuCas13a-Sumo-6 × his was gifted from Yanli Wang (Institute of Biophysics, Chinese Academy of Sciences, Beijing, China). Briefly, the plasmid was transferred into *Escherichia coli* (*E. coli*) Rosetta2 (DE3) cells on ice for 30 min. The vector was incubated at 42 °C for 90 s and then placed on ice for 10 min. The mixture was added to TB medium for pre-culturing and transferred to plate medium. After pre-expression, Strains with high expression evaluated by electrophoresis were selected for expanded cultivation and preservation. For preparation of the Cas13a, the highly expressed strain was added to TB broth medium containing 34 μg mL^{-1} chloramphenicol (Sangon) and 50 μg mL^{-1} kanamycin (Sangon) and incubated at 37 °C for 7.5 h to $OD_{600} = 0.6$, and cultured with 0.1 mM isopropyl-1-thio-b-D-galactopyranoside (IPTG) at 16 °C for 16 h. The bacteria were collected and broken by ultrasound with the buffer containing 20 mM Tris-HCl, pH 7.5, 500 mM NaCl, 10% glycerol. After centrifugation, the supernatant was incubated with Ni Sepharose (GE Healthcare), washed with the first washing containing 20 mM imidazole and eluted with the first elution buffer containing 500 mM imidazole at 4 °C. Then the eluted solution was digested with Ulp1 protease at 4 °C overnight to remove the 6His-Sumo tag and purified on a heparin column (Sangon) with the second washing containing 20 mM Tris-HCl, 1 M NaCl and 10% glycerol and the second elution buffer containing 20 mM Tris-HCl, pH 7.5, 1 M

NaCl and 10% glycerol. The resulting liquid was subjected to ultrafiltration with 50% glycerol to a final concentration of 1 mg/mL and was stored at −80 °C before use.

2.3. In vitro transcription and purification of CrRNA

Two complementary DNA oligonucleotide strands with T7 promoter and trigger sequence were annealed to form one double-stranded DNA at 94 °C for 5 min and slowly cooled to 25 °C at 0.1 °C/s. The annealed template DNA, T7 RNA polymerase, RNase inhibitor, NTP and reaction buffer containing 40 mM Tris-HCl, pH 7.9, 6 mM $MgCl_2$, 10 mM DTT, 10 mM NaCl and 2 mM Spermidine were incubated for 12 h at 37 °C to perform the transcription in vitro. Then DNase I and DNase I reaction buffers were added to the reaction solution and incubated at 37 °C for 1 h. The transcription products were purified by RNA clean Kit (TIAGEN). The concentration of CrRNA was measured by NanoDrop2000.

2.4. Fluorescent assay of Cas13a collateral cleavage activity

The LbuCas13a enzyme and CrRNA at a ratio of 2:1 were pre-incubated at room temperature for 10 min. After that, Trigger RNA, FQ6U reporter probe, DEPC-treated water and 10 × reaction buffer (100 mM Tris-HCl, pH 8.0, 500 mM KCl, 15 mM $MgCl_2$) were added to construct 50 μL total volume, with LbuCas13a at final 20 nM, CrRNA at 10 nM, trigger RNA at 50 pM and reporter probes at 200 nM. The mixed solution was incubated at 37 °C for 30 min, and the fluorescence signal was recorded every 1 min with Rotor-Gene Q real-time fluorescence quantitative PCR instrument. The mixture free of LbuCas13a was used as the blank control. The change rate of fluorescence intensity difference between the experimental group and blank one indicated the Cas13a collateral cleavage activity.

2.5. Gel electrophoresis validation of Cas13a collateral cleavage

The reaction mixture containing the target as mentioned as 2.4 and that free of the target both under the action of Cas13a were incubated at 37 °C for 10 min and 95 °C for 5 min, after that 20% nondenaturing polyacrylamide gel electrophoresis (PAGE) was performed to identify the reaction products with 1 × TBE buffer at 110 V for 60 min. The gel image was acquired under UV light (ChemDoc XRS, Bio-Rad) after staining with GelRed (Sangon) for 30 min.

2.6. Fluorescent assays of Cpccc

LbuCas13a enzyme was pre-incubated with CrRNA-T (specific to target) at room temperature for 10 min to form LbuCas13a/CrRNA-T complex, and the concentration ratio of LbuCas13a to CrRNA was 2:1. LbuCas13a/CrRNA-M (specific to product of the mediator) complex was formed under the same conditions. Target RNA, LbuCas13a/CrRNA-T, mediator, LbuCas13a/CrRNA-M, DEPC-treated water and 10 × reaction buffer (100 mM Tris-HCl, pH 8.0, 500 mM KCl, 15 mM $MgCl_2$) were mixed and incubated at 37 °C for 10 min. Finally, the reporter probe in10 μl was added to the system for the total of 50 μL. The fluorescence signal was immediately detected every 10 s by Rotor-Gene Q real-time fluorescence quantitative PCR instrument in green channel at 37 °C for 30 min.

2.7. Cell culture and total RNA extraction

The non-tumorigenic epithelial cell line (MCF-10A) was cultured in its special medium. The human breast cancer cell lines (MCF-7 and MDA-MB-231) and human hepatoma cell line (Hep-3B) were cultured in DMEM mediumwith 10% fetal bovine serum (FBS). The cells were incubated in a humidified incubator at 37 °C with 5% CO_2 before cell density reaches 70%–80%. Then the cells were dissociated and centrifuged for collection. According to the manufacturer's instructions, total RNA of the cultured cells was extracted using TRNzol Universal reagent. After that, the extracted total RNA was measured by Nanodrop 2000 to quantify the concentration and stored at −80 °C before use.

2.8. Extraction of virus RNA

The RNA of RSV was acquired from upper respiratory tract sputum samples taken from the patients at the Children's Hospital of Chongqing Medical University. In briefly, sputum specimens were inactivated at 55 °C for 20 min and digested with 4% NaOH for 15 min. After centrifugation, the precipitates were collected, washed with DEPC- treated water and the RNA was extracted with EZ-10 Spin Column Viral Total RNA Extraction Kit (Sangon, Shanghai) at room temperature following the instruction of the supplier. The acquired RNA was stored at −80 °C before use.

2.9. Quantitative real-time PCR experiment

The 20 μL reverse transcription (RT) reaction of miRNA-21 was performed with MiRNA Synthesis Kit of First Strand (Sangon, Shanghai) after adding 0.5 μM stem-loop RT primer and 2 μg extracted total small RNA (20–200 nt) from cell lines mentioned above. The mixture was incubated at 16 °C for 30 min and 37 °C for 30 min, followed by heating at 85 °C for 5 min. After 10 times dilution, 1 μL newly synthesized cDNA liquid was added to qPCR mixture to analyse the miRNA-21 expression. The 20 μL qPCR reaction was conducted by 2 × SYBR Green qPCR Master Mix Kit (Biomake, Shanghai) containing 10 μL of 2 × SYBR Green Master Mix, 1 μL of forward primer, 1 μL of reverse primer, 1 μL of RT product and 7 μL of RNase-free water. The qPCR reaction was carried out in CFX Connect Real-Time PCR Detection System at 94 °C for 1 min followed by 35 cycles of 94 °C for 5 s and 60 °C for 30 s, and then 72 °C for 10 min. The relative expression of cell samples was evaluated by referring to the expression of U6 gene using the $2^{-\Delta\Delta Ct}$ method.

The reverse transcription and qPCR reaction of RSV referred to that of miRNA-21 with some modification. In a word, we replaced the stem-loop RT with specific primers and conducted qPCR at 94 °C for 3 min followed by 39 cycles of 94 °C for 10 s and 60 °C for 30 s, and then 72 °C for 10 min.

3. Results and discussion

3.1. Principle of Cpccc

Cas13a in complex with CrRNA specific to target RNA exhibits a half-fist hollow conformation [42], which putatively reduces its steric hindrance, making intra-enzyme chain replacement of Cas13a possible, and we proved this in *3.4*.

The hybridization of target RNA with the variable region of CrRNA-T results in a double helix RNA with a rigid structure and the transformation of the half-fist conformation of Cas13a into a clenched fist conformation, which is the active form for non-specific *trans*-cleavage of single-stranded RNA with the efficiency as high as 10^3 and the preference for U > G > A = C. Because the target RNA activates the Cas13a/CrRNA-T complex at a ratio of 1:1 through hybridization [43], target RNA in trace abundance activates trace Cas13a that produce insignificant signal change. To achieve high sensitivity to detect trace levels of target RNA, the accumulation of the activated Cas13a is preferred over the PCR amplification of target RNA to decrease analysis time and facilitate operation. The Cas13a/CrRNA complex recognizes single-stranded RNA rather than double-stranded RNA. Based on the principle of branching chain migration, however, the chain replacement reaction driven by a toehold can putatively occur between Cas13a/CrRNA complex and double-stranded RNA, which was proved in 3.4. Hence, a suitable hairpin RNA strand can be designed as a mediator that is susceptible to cleavage by target RNA-activated Cas13a/CrRNA. The cleavage products function as the secondary target to recognize

CrRNA-M and activate the Cas13a/CrRNA-M complex, promoting the double cascade cyclic reaction and the accumulation of activated Cas13a for efficient cleavage of reporting RNA. In brief, the Cas13a/CrRNA-T complex recognizes and binds with target RNA, leading to the activation of Cas13a and the cleavage of mediator hairpin RNA for generating the secondary RNA as in double-strand with a toehold at the 5′-end. The secondary RNA binds to Cas13a/CrRNA-M through the chain replacement reaction and activates it to promote the mediator-based *trans*--cleavage and circular cascade activation of Cas13a. Finally, the accumulation of activated Cas13a and the efficient cleavage of reporting RNA are achieved for sensitive detection of target RNA (Fig. 1).

3.2. Expression of Cas13a and characterization of the collateral cleavage activity

LbuCas13a was expressed and purified, following the methods of a previous study with some modifications [42]. The purity of the enzyme was evaluated using sodium dodecyl sulfate-polyacrylamide gel electrophoresis (PAGE) (Fig. 2A). LbuCas13a with a molecular weight (MW) of 138.5 kDa was obtained with the purity >90% analyzed by Image Lab 3.0 (Fig. 2A in lanes 8 with increased quantities of elutes).

To assess the specificity recognition of Cas13a, miRNA-21 and miRNA-17 were used as the target and non-target models, respectively. We developed an analysis system to verify the collateral cleavage activity of the expressed LbuCas13a and its specific recognition. The CrRNA with the flexible region complementary to miRNA-21 was designed. A short single-stranded RNA was designed as the reporter probe, which contained six uracil residues with fluorescein (FAM) and black hole quencher at the 5′ and 3′ ends, respectively. The activation of Cas13a/CrRNA after the recognition and binding of the target RNA leads to the cleavage of the reporter probe, which results in FAM release and fluorescence signal generation. The 50 μL reaction mixture comprising 50 pM miRNA-21, 20 nM Cas13a, 10 nM CrRNA, and 200 nM RNA reporting probe was incubated at 37 °C for over 15 min. A typical enzyme reaction curve was observed (Fig. 2B). In the absence of target RNA, no significant changes in fluorescence signal were observed; the removal of any components resulted in changes in fluorescence intensity as those in the blank (Fig. 2B). The replacement of miRNA-21 with miRNA-17 resulted in negligible changes in fluorescence intensity. Thus, LbuCas13a exhibited target-specific activation and high activity for collateral cleavage of uracil-rich reporter RNA, which is beneficial for the recognition and detection of targets.

3.3. Design and optimization of mediator

To develop Cpccc, mediators were designed to simultaneously serve as cleavage substrates for target RNA-activated Cas13a/CrRNA-T and its product as the secondary target RNA for the enhanced activation of Cas13a/CrRNA-M. The mediator structure is crucial for the sensitivity, high specificity, low false-positive rates of Cpccc.

To enhance the sensitivity and specificity of Cpccc by utilizing the target-specific activation of Cas13a and its cleavage preference for uracil-comprising single-stranded RNA sequence [44], the hairpin structural mediator should have a uracil-comprising loop with a suitable number of non-complementary bases so that it can be cleaved preferentially at the uracil base by the activated Cas13a/CrRNA-T within a certain duration, resulting in a double-stranded RNA strand with a toehold. The double-stranded RNA recognizes the Cas13a/CrRNA-M

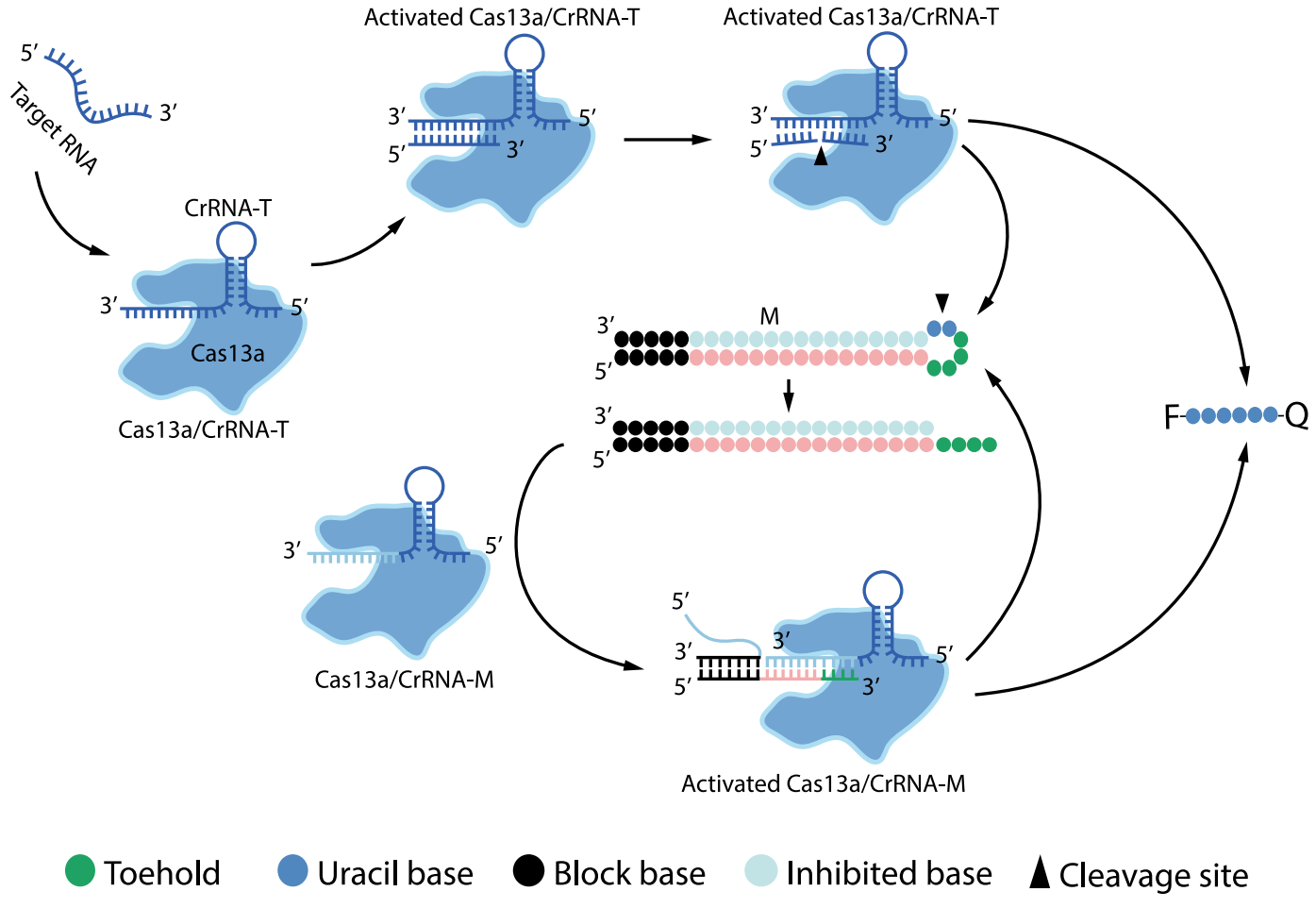


Fig. 1. Schematic illustration of Cpccc for rapid detection of RNA.

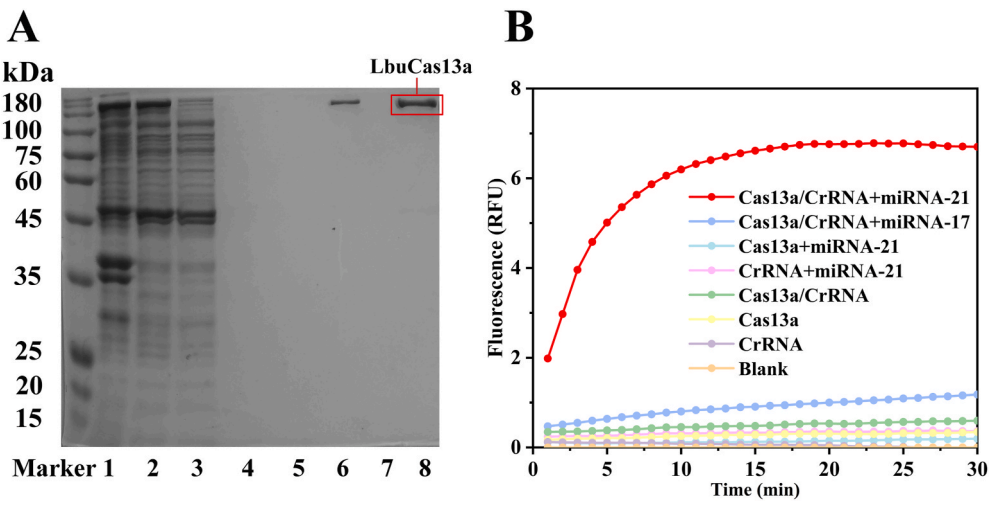


Fig. 2. Expression and activity analysis of Cas13a. (A) SDS-PAGE for the purification of LbuCas13a. Cell lysate (1), sediments (2), flow through fractions (3), first washing with 20 mM imidazole (4), the first eluant for 6His-Sumo-LbuCas13a with 500 mM imidazole (5), Ulp1-digesting product (6), the second washing with 20 mM Tris-HCl, 1 M NaCl and 10% glycerol (7), ultrafiltration eluant of LbuCas13a (8). (B) The collateral cleavage activity of Cas13a/CrRNA.

complex. The cleavage susceptibility of the mediator to the activated Cas13a/CrRNA-T and the high potency of the resultant product to recognize and activate Cas13a/CrRNA-M ensure sufficient sensitivity of Cpccc. More uracil residues in the loop will favor the cleavage but the resultant product will have limited number of bases complementary for Cas13a/CrRNA-M and suppresses the activation. Thus, only two adjacent uracil bases were adopted in the loop. To maintain minimal false-positive rates, the mediator should contain a suitable number of bases on the stem relative to that on the loop, which can inhibit the cleavage-independent unlocking of the loop and the resultant unexpected activation of Cas13a/CrRNA-M. The mediator along with the toehold is expected recognize and activate Cas13a/CrRNA-M through the chain replacement reaction of branch chain migration. Moreover, five additional base pairs were added to the end of the stem as a blocker. Thus, the number of bases on the loop and that on the stem should be optimized for achieving an ideal performance of Cpccc.

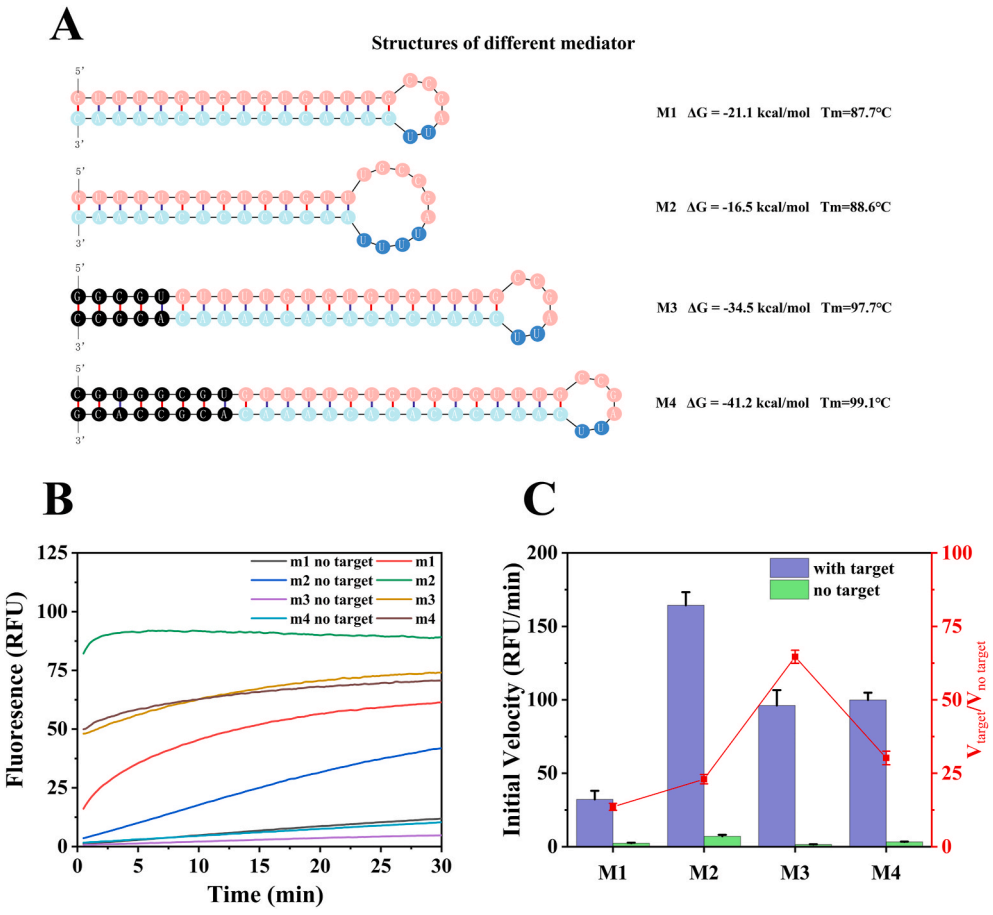


Fig. 3. Performance of different mediators. Different mediators with different structures (A), black represents the blocking base, pink represents the complementary base of CrRNA variable region, and blue represents the spliced base. Fluorescence intensity changes (B) and Fluorescence intensity change ratios (C) with different mediators for Cpccc. M1, M2, M3 and M4 represent different mediators. V_{target} and $V_{no\ target}$ represent the initial velocity of fluorescence growth of the test group and the control group, respectively. (For interpretation of the references to colour in this figure legend, the reader is referred to the Web version of this article.)

To demonstrate the proposed scheme, different mediators with different sequences including varied numbers of uracil in the loops and bases in hairpin structures shown in Fig. 3A and Supplementary Table S1 were comparatively analyzed, to select the optimal mediator with the high ratio of fluorescence intensity change rate to that of the target-free blanks.

The fluorescence intensity changes of Cpccc with different mediators were recorded from the initial 10 s after the mixing of the components (Fig. 3B). According to the ratio of fluorescence intensity of the test group to that of the corresponding target-free blanks (Fig. 3C), mediator-3 (M3) with the base number ratio in stem and loop at 16:6 and five base pairs at the end of stem as the blocker were selected for the experiments.

To achieve the ideal performance of Cpccc, the concentrations of M3, a key parameter, were optimized. Three concentrations of M3 (100, 150, and 200 pM) were used with 10 nM LbuCas13a/CrRNA-T, 10 nM LbuCas13a/CrRNA-M, and 50 pM target RNA. The reaction kinetics (Fig. 4A) and the initial velocity derived from the change in fluorescence intensity relative to that in the target-free blank (Fig. 4B) indicated that 150 pM of M3 was the optimal concentration. Theoretically, the low concentration of mediator will result in low levels of the cleaved product to activate Cas13a/CrRNA-M and consequently a weak change in fluorescence signal whereas a high concentration of the mediator can result in enhanced changes in the fluorescence signal on condition of the sufficient activated Cas13a/CrRNA-M. However, an increased change in the fluorescence signal of the blank was observed at a higher concentration of the mediator (Fig. 4A). We hypothesize that the proportion of unannealed mediators is not ignorable at high concentrations of mediators, which may result in the unexpected cyclic activation of Cas13a/CrRNA-M and increased the false-positive rates. In brief, we adjusted the low concentration of mediator in the system to keep false positives tiny, considering that too low concentration of mediator would affect the cyclic activation rate, so we took a tradeoff value.

3.4. Feasibility of Cpccc for RNA detection

To verify that the activated LbuCas13a cleaved only uracil bases on the loop but not the bases on the stem of the hairpin mediator within 10 min due to the double chain hindrance, the activated Cas13a/CrRNA-T-mediated cleavage of designed mediators was examined using non-denatured PAGE with a 20% gel. As shown in Fig. 5A, lane 3 containing all components showed two chains of low MW products when compared with lane 1 containing only mediator and lane 2 (lacks target). No fragments other than the two chains of low molecular weights were observed, revealing that only the double uracil bases on the loop of the mediator were cleaved. In contrast, lane 4 comprising non-target miRNA-17 and Cas13a/CrRNA-T showed the intact mediator. These results indicated that the mediator could be cleaved at uracil bases only in the presence of target RNA.

As far as we know, Cas13a targets single-stranded RNA rather than double chain target. For practice of Cpccc, it is imperative to prove the presence of intra-enzyme chain replacement. Thus, the potency of the cleaved mediator to activate Cas13a/CrRNA-M through the chain replacement reaction was examined. A double-stranded RNA containing a toehold at the end (designed to simulate the product of the cleaved mediator) and a single-stranded target of CrRNA-M (designed as the positive activator) was compared for activation of Cas13a/CrRNA-M. As shown in Fig. 5B, the simulated product significantly increased the fluorescence signals similar to the single-strand target of CrRNA-M. However, the fluorescence signals were not observed in the absence of the activator or the presence of M3. As we all known, single stranded RNA rather than double strands activates Cas13a. This result demonstrates that Cas13a can also be activated by the double strand RNA with toehold. Considering the half-fist hollow structure of Cas13a/CrRNA, it can be reasonably explained that strand displacement reaction between toehold containing double RNA and variable regions of CrRNA achieves dissociation of the active chain part and the obstructing chain part in the double chain RNA while complementation of the active chain part and variable regions of CrRNA. In essence, the hollow structure of the Cas13a/CrRNA reduces steric hindrance and enables chain displacement between the toehold contained double strand RNA and the variable region of CrRNA, thus enabling the conversion of the double strand RNA to the single strand and activating Cas13a/CrRNA-M.

Furthermore, the feasibility of Cpccc was demonstrated using real-time fluorescence detection. The changes in fluorescence signals of Cpccc using the optimized mediator M3 (150 pM) for the Cpccc system in the presence of 50 pM target RNA were compared with the Cas13a-based directed detection (Fig. 5C). Cpccc exhibited maximum fluorescence intensity and initial velocity higher than Cas13a-based direct detection. It can be easily found that Cpccc is more efficient than Cas13a-based direct detection. The secondary directed detection promoted only by M3 exhibited insignificant changes in fluorescence intensity, indicating low false-positive rates by M3 under these conditions for Cpccc. Thus, M3 was demonstrated as a potent mediator. However, the expected exponential response curve for a typical enzyme was not observed under these conditions. This suggested the need for a higher concentration ratio of mediator to LbuCas13a/CrRNA or further optimization of the mediator structures. Theoretically, the exponential change of Cpccc is reachable with higher concentrations of mediators. However, higher concentrations of mediators will result in higher false-positive rates, especially with the target RNA at low levels to initiate the LbuCas13a/CrRNA-T for the primary collateral cleavage. Thus, the proposed system for Cpccc was feasible and these conditions were

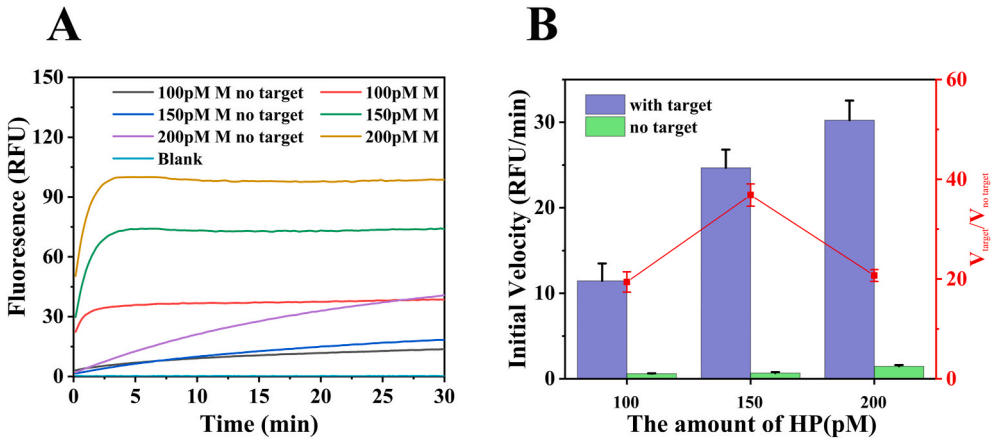


Fig. 4. Optimization of mediator concentration. Fluorescence intensity changes (A) and relative initial velocity (B) of Cpccc with different concentrations of M3. V_{target} and $V_{no\ target}$ represent the initial velocity of fluorescence growth of the test group and the control group, respectively.

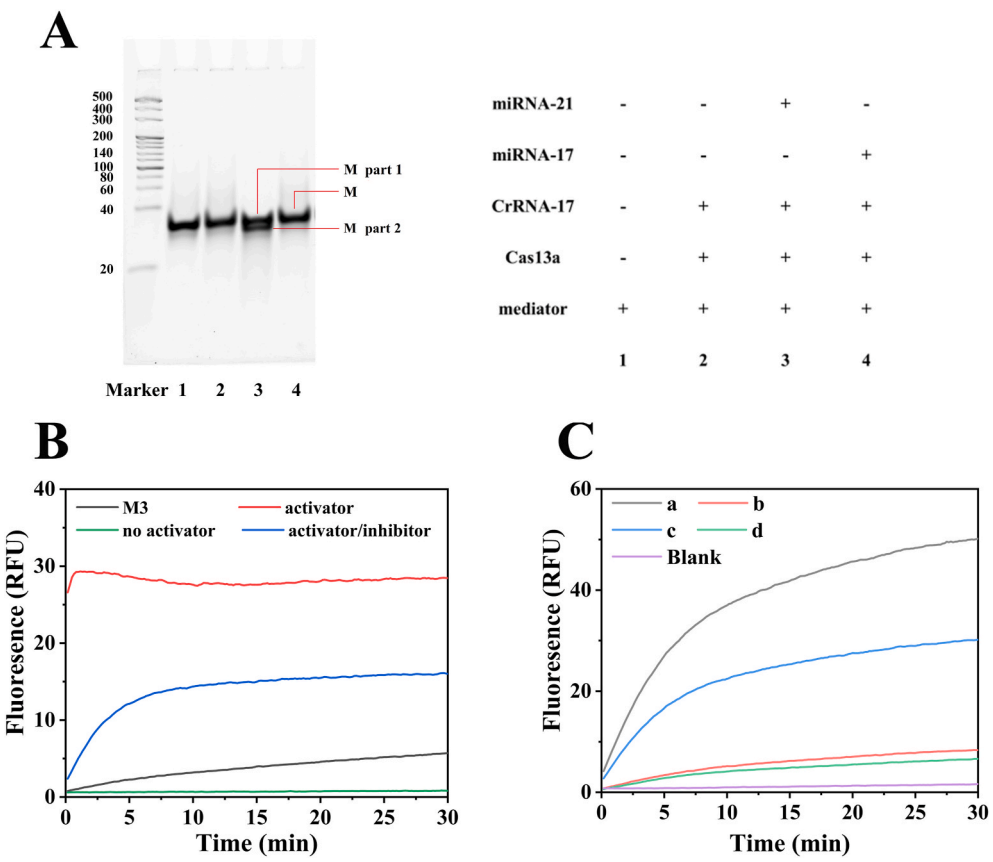


Fig. 5. Feasibility of Cpccc for miRNA detection. (A) 20% non-denatured PAGE gel electrophoresis of mediator. The left part is electrophoretic gel, and the right part is element of every lane. (B) Fluorescence changes of sliced mediator activation. M3: mediator, activator: the designed single-strand target; activator/inhibitor: the designed simulate of the cleaved product of mediator; no activator: the negative control group. (C) Fluorescence changes of Cpccc for miRNA-21 detection. Five groups including Cpccc (a), Cpccc with no target (b), Cas13a-based direct detection (c) and M3 direct activation (d).

optimal for the detection of RNA at low levels.

3.5. Sensitivity of Cpccc for RNA detection

The sensitivity of the Cpccc system depends on the *trans*-cleavage activity of Cas13a and signal amplification by the mediator-based cascade cyclic activation of Cas13a. In this study, the sensitivity of the designed system was examined using miRNA-21 and its CrRNA-T. Under the optimized conditions, the fluorescence intensity and initial velocity were linearly correlated with miRNA-21 from 10 fM to 50 pM (R^2 = 0.9819) (Fig. 6). The LOD (defined as the ratio of three times the standard deviation of three replicates of the control sample without target to the slope of the linear response) and the limit of quantification (defined as the sum of LOD and five times the standard deviation of the predicted values from the linear regression) were 75 aM and 8.1 fM, respectively. This indicated that the Cpccc system exhibited low LOD and high sensitivity.

3.6. Specificity of Cpccc for miRNA detection

The target miRNA-21 was replaced with miRNA-17, miRNA-141, and miRNA-29a to examine the specificity of the Cpccc system comprising LbuCas13a/CrRNA-T. The fluorescence intensity (Fig. 7a) and initial velocities (Fig. 7b) in the reaction mixture comprising miRNA-17, miRNA-141, and miRNA-29a were similar to those in the blank. Meanwhile, the analysis of the reaction mixture comprising

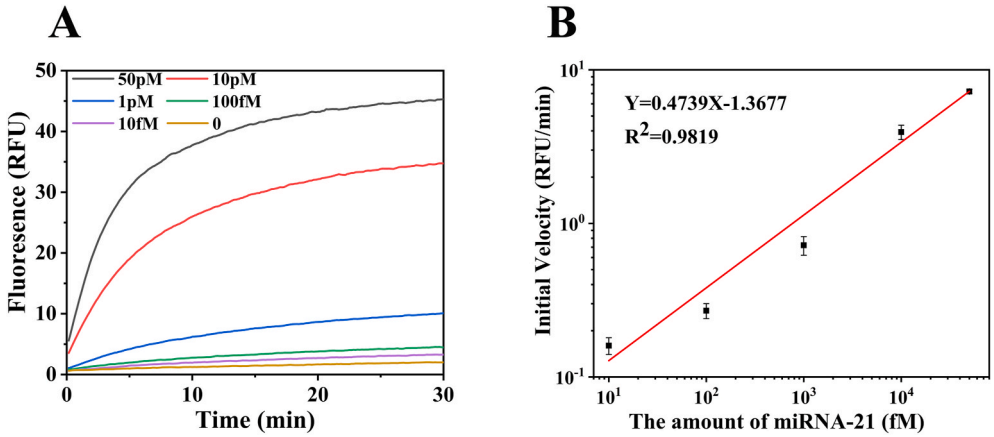


Fig. 6. Sensitivity of Cpccc for the detection of RNA. Fluorescence intensity of Cpccc in response to the concentrations of miRNA-21(A); initial velocity plots of Cpccc for detection of miRNA-21 (B). Error bars indicate one standard deviation of triplicated independent tests.

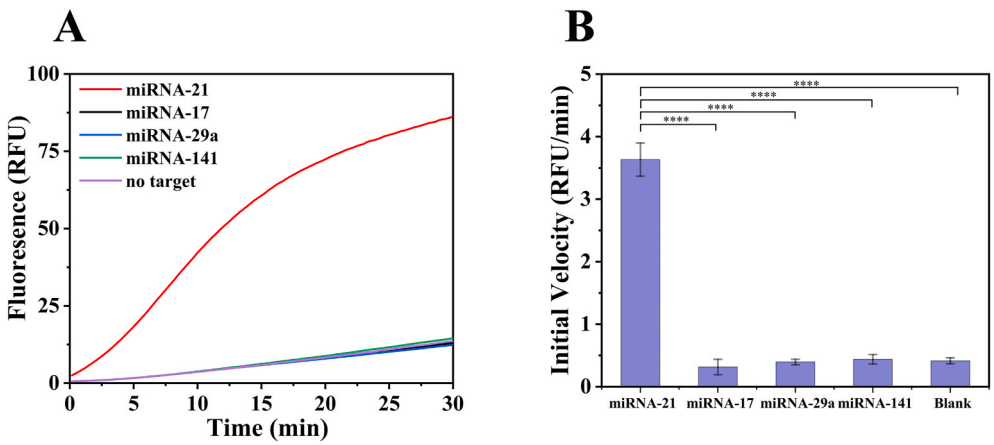


Fig. 7. Specificity evaluation of the strategy for miRNA detection. Fluorescence intensity Changes(A) and initial velocity of Cpccc for detecting different miRNA(B) (n = 3 technical replicates, two-tailed Student *t*-test; ****, p < 0.0001).

miRNA-21 at 50 pM using the Cpccc system revealed markedly increased changes in fluorescent intensity and initial velocity. Thus, the proposed Cpccc was demonstrated to exhibit high specificity for RNA detection.

3.7. Application of Cpccc

To evaluate the applicability of the proposed strategy in complex biological samples, The nontumorigenic epithelial cell line (MCF-10A), human breast cell lines (MCF-7 and MDA-MB-231) and human hepatoma cell line (Hep-3B), were cultured and miRNA-21 derived from extracts of those cells were tested. As shown in Fig. 8A, the expressions of the miRNA-21 in the cancer cells are higher than that in the normal cells, consistent with the result quantified by RT-qPCR. These results are in according with previous studies [45].

To evaluate the reliability of Cpccc for detection RSV in clinical samples, results of four patient samples and one sample from healthy person by Cpccc and qRT-PCR were compared. As shown in Fig. 8B, the heatmap of the normalized signal intensities demonstrates consistent results of Cpccc and qRT-PCR. To further evaluate the applicability of the Cpccc system, six RSV-positive and six RSV-negative clinical sputum specimens (confirmed with the fluorescence immunoassay in clinic) were applied for the Cpccc system. The analysis results are shown in Fig. 8C. To identify the RSV-positive samples, the sum of mean values and 1.96 times the standard deviation of healthy samples were used as the threshold value. The values in the RSV-positive samples were higher than the threshold value. The results of analysis with the Cpccc system were consistent with those of fluorescence immunoassay in clinical test.

4. Conclusions

In this study, we proposed a Cpccc system without PCR for rapid, sample, highly sensitive, and specific detection of RNA. The detection of RSV in clinical sputum specimens also confirmed the performance of Cpccc. Based on the uracil preference of *trans*-cleavage by the activated LbuCas13a, the uracil-containing hairpin mediator was designed not only as the substrate of the target-initiated first *trans*-cleavage of Cas13a/CrRNA-T but also its product as the secondary target to recognize and initiate the cascade *trans*-cleavage of Cas13a/CrRNA-M.

Most importantly, it is broadly known that Cas13a targets single-stranded RNA rather than double chain RNA. here we found that double-stranded RNA with a toehold also can activate Cas13a, which may expand the application paradigms of Cas13a. The activation mechanism is putatively that the repressed Cas13a/CrRNA with a half-fist hollow conformation provides wabbly space to the variable region of CrRNA, which reduces its steric hindrance, making intra-enzyme

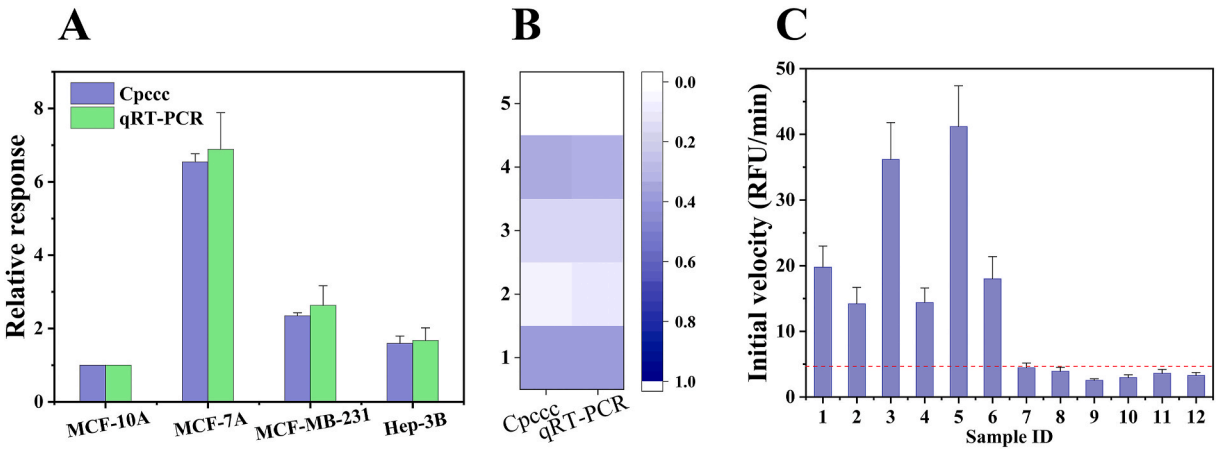


Fig. 8. Application performance of the strategy. Compare the results for the relative expression of miRNA-21 by Cpccc and qRT-PCR methods (A). Four groups were cell line extracts of MCF-10A, MCF-7A, MCF-MB-231 and Hep-3B. Heatmap of the normalized signal intensities of four patient samples marked 1–4 and one sample from healthy person marked 5 in Cpccc and qRT-PCR. Data represent means (B). Histograms of the initial rate of the fluorescence signal for clinical samples detection by Cpccc (C). The sputum samples marked as 7–12 from healthy person gave threshold value of mean + 1.96SD (in red dashed line) and other 6 sputum samples marked as 1–6 involved 6 positive clinical sputum samples. (For interpretation of the references to colour in this figure legend, the reader is referred to the Web version of this article.)

chain replacement of Cas13a possible. It is the Cas13a amplification effect and the continuous accumulation of activated Cas13a that endow the sensitivity with LOD of 75 aM, the high selectivity of Cas13a contributes to the high specificity, and the facility for target RNA detection was achieved with only one enzyme, one mediator, two complexes for reaction with a maximum duration of 30 min, and in a "mix & read" mode even in room temperature. The proposed Cpccc system can be used to detect various RNAs using customized CrRNA.

This is the first Cas13a-based cascade cyclic RNA detection study without PCR for as rapid as 0.5 h, and conveniently applicable for microfluidic detection. Comparing with 100–10 fM target concentration detectable of direct Cas13a-based RNA detection [44], the proposed Cpccc strategy realized as low as 75aM of LOD without amplification in 30min owing to the cascade cycle and subsequently continuous accumulation of activated Cas13a, which further expanded the application of Cas13a.

Considering the unrealized expectant exponential curve for the reaction potency, the sensitivity and specificity of the proposed system can be further improved by optimizing the structures of the mediators. In summary, this novel Cpccc system that can detect RNA viruses with high sensitivity in the "mix & read" mode at room temperature is a rapid, simple, convenient, and highly sensitive method for RNA detection. The Cpccc system has potential applications in point-of-care testing and high throughput screening of RNA virus infections.

CRediT authorship contribution statement

Hongwei Zeng: Conceptualization, Methodology, Software, Validation, Formal analysis, Investigation, Data curation, Writing – original draft, Visualization. **Penghui Zhang:** Investigation, Resources. **Xue Jiang:** Investigation, Resources. **Changyuan Duan:** Software, Investigation. **Yang Yu:** Investigation, Resources. **Qiaoming Wu:** Investigation. **Xiaolan Yang:** Resources, Methodology, Supervision, Formal analysis, Writing – review & editing, Project administration, Funding acquisition.

Declaration of competing interest

The authors declare that they have no known competing financial interests or personal relationships that could have appeared to influence the work reported in this paper.

Acknowledgments

This work is supported by National Natural Science Foundation of China (grant no.31570862), Natural Science Foundation Project of Chongqing (CSTC2012JJA0057, CSTC2019jcyj-msxmX0166). We give special thanks to Professor Yanli Wang from the Institute of Biophysics, Chinese Academy of Sciences for supply of the pET-28a-LbuCas13a-Sumo-6 × his expression vectors.

Appendix A. Supplementary data

Supplementary data to this article can be found online at https://doi.org/10.1016/j.aca.2022.340009.

References

[1] L.S. Kristensen, M.S. Andersen, L.V.W. Stagsted, K.K. Ebbesen, T.B. Hansen, J. Kjems, The biogenesis, biology and characterization of circular RNAs, Nat. Rev. Genet. 20 (11) (2019) 675–691.
[2] D. Trzybulska, E. Vergadi, C. Tsatsanis, miRNA and other non-coding RNAs as promising diagnostic markers, Ejifcc 29 (3) (2018) 221–226.
[3] D.P. Bartel, MicroRNAs: target recognition and regulatory functions, Cell 136 (2) (2009) 215–233.
[4] M. Zaratiegui, D.V. Irvine, R.A. Martienssen, Noncoding RNAs and gene silencing, Cell 128 (4) (2007) 763–776.
[5] T. Nguyen, D.D. Bang, A. Wolff, 2019 novel coronavirus disease (COVID-19): paving the road for rapid detection and point-of-care diagnostics, Micromachines 11 (3) (2020).
[6] A.P. Thrift, H.B. El-Serag, F. Kanwal, Global epidemiology and burden of HCV infection and HCV-related disease, Nat. Rev. Gastroenterol. Hepatol. 14 (2) (2017) 122. U68.
[7] N. Zhang, L. Wang, X. Deng, R. Liang, M. Su, C. He, L. Hu, Y. Su, J. Ren, F. Yu, L. Du, S. Jiang, Recent advances in the detection of respiratory virus infection in humans, J. Med. Virol. 92 (4) (2020) 408–417.
[8] D.S. Hui, E.I. Azhar, Y.-J. Kim, Z.A. Memish, M.-d. Oh, A. Zumla, Middle East respiratory syndrome coronavirus: risk factors and determinants of primary, household, and nosocomial transmission, Lancet Infect. Dis. 18 (8) (2018) E217–E227.
[9] N.D. Grubaugh, J.T. Ladner, P. Lemey, O.G. Pybus, A. Rambaut, E.C. Holmes, K. G. Andersen, Tracking virus outbreaks in the twenty-first century, Nat. Microbiol. 4 (1) (2019) 10–19.
[10] J.B. Varkey, J.G. Shantha, I. Crozier, C.S. Kraft, G.M. Lyon, A.K. Mehta, G. Kumar, J.R. Smith, M.H. Kainulainen, S. Whitmer, U. Stroeher, T.M. Uyeki, B.S. Ribner, S. Yeh, Persistence of Ebola virus in ocular fluid during convalescence, N. Engl. J. Med. 372 (25) (2015) 2423–2427.
[11] M. Ding, C. Wang, X. Lu, C. Zhang, Z. Zhou, X. Chen, C.-Y. Zhang, K. Zen, C. Zhang, Comparison of commercial exosome isolation kits for circulating exosomal microRNA profiling, Anal. Bioanal. Chem. 410 (16) (2018) 3805–3814.
[12] J.B. Mahony, Nucleic acid amplification-based diagnosis of respiratory virus infections, Expert Rev. Anti-infect. Ther. 8 (11) (2010) 1273–1292.
[13] S. Duffy, Why are RNA virus mutation rates so damn high? PLoS Biol. 16 (8) (2018).
[14] B.S. Batule, Y. Seok, M.-G. Kim, Paper-based nucleic acid testing system for simple and early diagnosis of mosquito-borne RNA viruses from human serum, Biosens. Bioelectron. 151 (2020).
[15] J. Tram, P. Le Baccon-Sollier, K. Bollore, J. Ducos, A.-M. Mondain, P. Pastor, G.-P. Pageaux, A. Makinson, P. Van de Perre, E. Tuaillon, RNA testing for the diagnosis of acute hepatitis A during the 2017 outbreak in France, J. Viral Hepat. 27 (5) (2020) 540–543.
[16] Y. Shen, F. Tian, Z. Chen, R. Li, Q. Ge, Z. Lu, Amplification-based method for microRNA detection, Biosens. Bioelectron. 71 (2015) 322–331.
[17] R. Huang, L. He, S. Li, H. Liu, L. Jin, Z. Chen, Y. Zhao, Z. Li, Y. Deng, N. He, A simple fluorescence aptasensor for gastric cancer exosome detection based on branched rolling circle amplification, Nanoscale 12 (4) (2020) 2445–2451.
[18] R.-D. Li, B.-C. Yin, B.-C. Ye, Ultrasensitive, colorimetric detection of microRNAs based on isothermal exponential amplification reaction-assisted gold nanoparticle amplification, Biosens. Bioelectron. 86 (2016) 1011–1016.
[19] B. Deiman, P. van Aarle, P. Sillekens, Characteristics and applications of nucleic acid sequence-based amplification (NASBA), Mol. Biotechnol. 20 (2) (2002) 163–179.
[20] L. Kang, J. Duan, F. He, J. Teng, J. Li, T. Yang, N. Luo, J. Zhao, S. Ding, W. Cheng, Highly sensitive fluorescence biosensing of BCR-ABL1 fusion gene based on exponential transcription-triggered hemin catalysis, Talanta 224 (2021).
[21] Y. Shan, X. Zhou, R. Huang, D. Xing, High-fidelity and rapid quantification of miRNA combining crRNA programmability and CRISPR/Cas13a trans-cleavage activity, Anal. Chem. 91 (8) (2019) 5278–5285.
[22] R. Barrangou, C. Fremaux, H. Deveau, M. Richards, P. Boyaval, S. Moineau, D. A. Romero, P. Horvath, CRISPR provides acquired resistance against viruses in prokaryotes, Science 315 (5819) (2007) 1709–1712.
[23] K.S. Makarova, Y.I. Wolf, J. Iranzo, S.A. Shmakov, O.S. Alkhnbashi, S.J.J. Brouns, E. Charpentier, D. Cheng, D.H. Haft, P. Horvath, S. Moineau, F.J.M. Mojica, D. Scott, S.A. Shah, V. Siksnys, M.P. Terns, C. Venclovas, M.F. White, A.F. Yakunin, W. Yan, F. Zhang, R.A. Garrett, R. Backofen, J. van der Oost, R. Barrangou, E. V. Koonin, Evolutionary classification of CRISPR-Cas systems: a burst of class 2 and derived variants, Nat. Rev. Microbiol. 18 (2) (2020) 67–83.
[24] J. McGinn, L.A. Marraffini, Molecular mechanisms of CRISPR-Cas spacer acquisition, Nat. Rev. Microbiol. 17 (1) (2019) 7–12.
[25] J.E. van Dongen, J.T.W. Berendsen, R.D.M. Steenbergen, R.M.F. Wolthuis, J.C. T. Eijkel, L.I. Segerink, Point-of-care CRISPR/Cas nucleic acid detection: recent advances, challenges and opportunities, Biosens. Bioelectron. 166 (2020).
[26] W. Zhou, L. Hu, L. Ying, Z. Zhao, P.K. Chu, X.-F. Yu, A CRISPR-Cas9-triggered strand displacement amplification method for ultrasensitive DNA detection, Nat. Commun. 9 (2018).
[27] J.S. Gootenberg, O.O. Abudayyeh, M.J. Kellner, J. Joung, J.J. Collins, F. Zhang, Multiplexed and portable nucleic acid detection platform with Cas13, Cas12a, and Csm6, Science 360 (6387) (2018) 439–+.
[28] G. Aquino-Jarquin, CRISPR-Cas14 is now part of the artillery for gene editing and molecular diagnostic, Nanomed. Nanotechnol. Biol. Med. 18 (2019) 428–431.
[29] C. Myhrvold, C.A. Freije, J.S. Gootenberg, O.O. Abudayyeh, H.C. Metsky, A. F. Durbin, M.J. Kellner, A.L. Tan, L.M. Paul, L.A. Parham, K.F. Garcia, K.G. Barnes, B. Chak, A. Mondini, M.L. Nogueira, S. Isern, S.F. Michael, I. Lorenzana, N. L. Yozwiak, B.L. MacInnis, I. Bosch, L. Gehrke, F. Zhang, P.C. Sabeti, Field-deployable viral diagnostics using CRISPR-Cas13, Science 360 (6387) (2018) 444–448.
[30] J.S. Chen, E. Ma, L.B. Harrington, M. Da Costa, X. Tian, J.M. Palefsky, J.A. Doudna, CRISPR-Cas12a target binding unleashes indiscriminate single-stranded DNase activity, Science 360 (6387) (2018) 436–+.
[31] D. Wang, S. He, X. Wang, Y. Yan, J. Liu, S. Wu, S. Liu, Y. Lei, M. Chen, L. Li, J. Zhang, L. Zhang, X. Hu, X. Zheng, J. Bai, Y. Zhang, Y. Zhang, M. Song, Y. Tang, Rapid lateral flow immunoassay for the fluorescence detection of SARS-CoV-2 RNA, Nat. Biomed. Eng. 4 (12) (2020) 1150–1158.

[32] P. Qin, M. Park, K.J. Alfson, M. Tamhankar, R. Carrion, J.L. Patterson, A. Griffiths, Q. He, A. Yildiz, R. Mathies, K. Du, Rapid and fully microfluidic Ebola virus detection with CRISPR-cas13a, ACS Sens. 4 (4) (2019) 1048–1054.
[33] R. Bruch, J. Baaske, C. Chatelle, M. Meirich, S. Madlener, W. Weber, C. Dincer, G. A. Urban, CRISPR/Cas13a-Powered electrochemical microfluidic biosensor for nucleic acid amplification-free miRNA diagnostics, Adv. Mater. 31 (51) (2019).
[34] Y. Liu, H. Xu, C. Liu, L. Peng, H. Khan, L. Cui, R. Huang, C. Wu, S. Shen, S. Wang, W. Liang, Z. Li, B. Xu, N. He, CRISPR-Cas13a nanomachine based simple technology for avian influenza A (H7N9) virus on-site detection, J. Biomed. Nanotechnol. 15 (4) (2019) 790–798.
[35] H. Khan, A. Khan, Y. Liu, S. Wang, S. Bibi, H. Xu, Y. Liu, S. Durrani, L. Jin, N. He, T. Xiong, CRISPR-Cas13a mediated nanosystem for attomolar detection of canine parvovirus type 2, Chin. Chem. Lett. 30 (12) (2019) 2201–2204.
[36] Y. Chang, Y. Deng, T. Li, J. Wang, T. Wang, F. Tan, X. Li, K. Tian, Visual detection of porcine reproductive and respiratory syndrome virus using CRISPR-Cas13a, Trans. Emerg. Dis. 67 (2) (2020) 564–571.
[37] Y. He, Y. Wu, Y. Wang, X. Wang, S. Xing, H. Li, S. Guo, X. Yu, S. Dai, G. Zhang, M. Zeng, W. Liu, Applying CRISPR/Cas13 to construct exosomal PD-L1 ultrasensitive biosensors for dynamic monitoring of tumor progression in immunotherapy, Adv. Therapeut. 3 (10) (2020), 2000093. Article No.: 2000093.
[38] T. Zhou, R. Huang, M. Huang, J. Shen, Y. Shan, D. Xing, CRISPR/Cas13a powered portable electrochemiluminescence chip for ultrasensitive and specific MiRNA detection, Adv. Sci. 7 (13) (2020).
[39] M. Huang, R. Huang, H. Yue, Y. Shan, D. Xing, Ultrasensitive and high-specific microRNA detection using hyper-branching rolling circle amplified CRISPR/Cas13a biosensor, Sensor. Actuator. B Chem. 325 (2020).
[40] X. Wang, S. Zhou, C. Chu, M. Yang, D. Huo, C. Hou, Target-induced transcription amplification to trigger the trans-cleavage activity of CRISPR/Cas13a (TITAC-Cas) for detection of alkaline phosphatase, Biosens. Bioelectron. 185 (2021).
[41] K. Shi, S. Xie, R. Tian, S. Wang, Q. Lu, D. Gao, C. Lei, H. Zhu, Z. Nie, A CRISPR-Cas autocatalysis-driven feedback amplification network for supersensitive DNA diagnostics, Sci. Adv. 7 (5) (2021).
[42] L. Liu, X.Y. Li, J. Ma, Z.Q. Li, L.L. You, J.Y. Wang, M. Wang, X.Z. Zhang, Y.L. Wang, The molecular architecture for RNA-guided RNA cleavage by Cas13a, Cell 170 (4) (2017) 714–+.
[43] A. East-Seletsky, M.R. O'Connell, S.C. Knight, D. Burstein, J.H.D. Cate, R. Tjian, J. A. Doudna, Two distinct RNase activities of CRISPR-C2c2 enable guide-RNA processing and RNA detection, Nature 538 (7624) (2016) 270–+.
[44] A. East-Seletsky, M.R. O'Connell, D. Burstein, G.J. Knott, J.A. Doudna, RNA targeting by functionally orthogonal type VI-A CRISPR-cas enzymes, Mol. Cell 66 (3) (2017) 373–+.
[45] X. Li, D. Zhang, X. Gan, P. Liu, Q. Zheng, T. Yang, G. Tian, S. Ding, Y. Yan, A cascade signal amplification based on dynamic DNA nanodevices and CRISPR/Cas12a trans-cleavage for highly sensitive MicroRNA sensing, ACS Synth. Biol. 10 (6) (2021) 1481–1489.